

Coherence of gamma-band EEG activity as a basis for associative learning

Wolfgang H. R. Miltner*, Christoph Braun†, Matthias Arnold‡, Herbert Witte‡ & Edward Taub§

* Department of Biological and Clinical Psychology, Institute of Psychology, Friedrich-Schiller-University, Am Steiger 3/1, D-07743 Jena, Germany

† Institute of Medical Psychology and Behavioral Neuroscience, Eberhard-Kals-University, Hoppe-Seyler-Str. 3, D-72076 Tübingen, Germany

‡ Institute of Medical Statistics, Informatics, and Documentation, Friedrich-Schiller-University, Jahnstraße 1, D-07743 Jena, Germany

§ Department of Psychology, University of Alabama at Birmingham, Birmingham, Alabama 35294, USA

Different regions of the brain must communicate with each other to provide the basis for the integration of sensory information, sensory-motor coordination and many other functions that are critical for learning, memory, information processing, perception and the behaviour of organisms. Hebb¹ suggested that this is accomplished by the formation of assemblies of cells whose synaptic linkages are strengthened whenever the cells are activated or 'ignited' synchronously. Hebb's seminal concept has intrigued investigators since its formulation, but the technology to demonstrate its existence had been lacking until the past decade. Previous studies have shown that very fast electroencephalographic activity in the gamma band (20–70 Hz) increases during, and may be involved in, the formation of percepts and memory^{2–6}, linguistic processing⁷, and other behavioural and preceptual functions^{8–12}. We show here that increased gamma-band activity is also involved in associative learning. In addition, we find that another measure, gamma-band coherence, increases between regions of the brain that receive the two classes of stimuli involved in an associative-learning procedure in humans. An increase in coherence could fulfil the criteria required for the formation of hebbian cell assemblies¹, binding together parts of the brain that must communicate with one another in order for associative learning to take place. In this way, coherence may be a signature for this and other types of learning.

The subjects were 16 (9 female) healthy, right-handed (Edinburgh test of handedness¹³) student volunteers, aged between 22 and 36 years. Before participation, subjects were informed about all aspects of the experiment in accordance with the Helsinki Convention on human experimentation, and all signed an informed consent. The experimental protocol was approved by the institution's ethics committee.

In the associative-learning phase of the experiment, there were 60 trials in which a room-illuminating light of 3-s duration and of one colour (CS⁺), either red or green, was accompanied at its termination by an electric shock (an unconditioned stimulus (UCS)) delivered to either the dominant (8 subjects) or the non-dominant (8 subjects) mid-volar tip of the third digit. These trials were interspersed randomly with 60 trials in which a light of the alternate colour was presented for 3 s without noxious stimulation (CS⁻). The colour of CS⁺ was counterbalanced across subjects. The intertrial interval was 4 s. After the 120 acquisition trials, an extinction series of 80 trials was given in which 40 CS⁺ stimuli without electric shock and 40 CS⁻ stimuli were given in random order.

Figure 1 shows the sites of the scalp electrodes from which recordings were made. The abundance of gamma activity increased at all occipital and parietal electrode sites in CS⁺ and CS⁻ for the first 2 s of the trial period, after which it stayed at approximately the same elevated level for the last second of the trial ($F(5, 55) = 10.54$, $P < 0.003$). For the first 2 s of the trial there was a trend for gamma

abundance to be significantly greater in CS⁺ than in CS⁻ ($0.06 > P > 0.05$).

Arrows connect the 13 pairs of electrode sites for which an analysis of variance showed that gamma coherence in the 37–43-Hz band was significantly greater during CS⁺ trials than during CS⁻ trials ($P \leq 0.06$) for the 250-ms time window just before UCS onset (Fig. 1). When shock was delivered to the non-dominant (left) hand (Fig. 1a), four electrode pairs spanning the primary and association visual cortices, which receive visual input concerning CS⁺ and CS⁻, and the contralateral (right) or midline pericentral cortex, which receives input from the finger to which the electric shock was applied, exhibited greater gamma coherence during CS⁺ than during CS⁻, as did two electrode pairs connecting visual cortex with the contralateral posterior parietal somatosensory association area. No electrode pairs connecting visual cortex and the ipsilateral (left) pericentral cortex showed increased coherence. When shock was delivered to the dominant (right) hand (Fig. 1b), the laterality of increased coherence reversed. Five electrode pairs spanning the visual and left or midline pericentral cortex showed significantly increased coherence, as did two electrode pairs spanning visual and left posterior parietal cortices, whereas no electrode pairs connecting visual cortex and right pericentral cortex showed increased coherence. Thus, the pericentral and posterior parietal electrode sites showing a significant effect were either midline or in the hemisphere representing the finger receiving the electric shock. This temporal and stimulus specificity in combination with the topographic specificity exhibited with respect to the laterality of the UCS presentation indicates that a general attention and/or arousal effect is unlikely to produce these results, as noted in a previous review¹⁴. In the frequencies above and below the 37–43-Hz band there was an abrupt drop-off of electrode pairs exhibiting significant coherence, with approximately half or less than half the number found over the range 37–43-Hz. In the 30–37-Hz range, seven electrode pairs showed significant coherence, three when the shock was delivered to the left hand (one extending anomalously from occipital cortex to the left side of the brain) and four when the shock was delivered to the right hand (one anomalous). In the 43–48-Hz range, five electrode pairs showed significantly increased coherence, two with shock to the left hand (one anomalous) and three with shock to the right hand. Thus, the main focus of coherent gamma activity was in the 37–43-Hz band.

Gamma coherence was not greater in CS⁺ than CS⁻ during, first, the 250-ms time window early in the trial (1,250–1,500 ms after CS

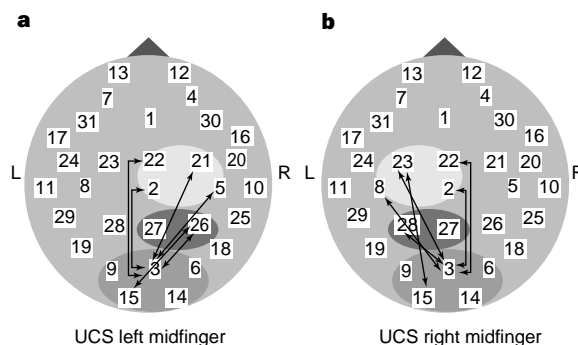


Figure 1 Pairs of electrode sites displaying significantly greater coherence in the 37–43-Hz gamma band during CS⁺ than during CS⁻ trials in the 2,750–3,000-ms time window for the 120 acquisition trials. Data are pooled for all subjects in a group. **a**, Arrows connect the electrode pairs showing this effect for a shock delivered to the non-dominant hand; **b**, arrows show the gamma-coherence connections for shock delivery to the dominant hand. The differently shaded ovals denote the approximate locations of the visual cortex (rear; intermediately shaded ovals) and of the two somatosensory association (middle, darkly shaded ovals) and two primary somatosensory (front; lightly shaded ovals) cortices representing the (left or right) hand receiving the electric shock.

onset); second, the last five trials of the 80-trial extinction period (during which the shock was never presented); or third, the last 30 CS⁺ and 30 CS⁻ trials of the extinction period for the pairs of electrodes (one left and one right) covering the somatosensory/visual cortex site (3–5 and 3–8, respectively) which showed particularly strong gamma-coherence conditioning effects. Gamma coherence therefore showed a specificity of effect to that part of the trial period and training/extinction series when the UCS was presented.

Increased coherence during the trial period was limited for other frequency bands in the electroencephalographic (EEG) spectrum. There was no greater coherence in CS⁺ than in CS⁻ for any electrode pair for the delta, theta or beta bands. For the alpha 1 band, two electrode pairs showed greater coherence in CS⁺ than in CS⁻; both extended from visual cortex to somatosensory association (but not primary somatosensory) cortex, one to the side representing the finger receiving the UCS and the other to the side representing the unstimulated finger. The latter, anomalous linkage was the only one that showed a significant effect for the alpha 2 band. There was no significant increase in coherence between any electrode pairs in the 80–100-Hz range ($F(1, 15) = 0.21$, not significant), indicating that the results were not due to an artefact of 'spillover' muscle activity.

Our observation of increased gamma coherence during the time window preceding the application of the UCS in CS⁺ trials was specific to the application of time-varying autoregressive modelling of the multivariate time series, which is based on Kalman filtering¹⁵ where coherence measures are estimated adaptively. When we applied conventional coherence methods using cross-spectral analysis based on the fast Fourier transform (FFT) or wavelet analysis, similar results could not be obtained. Presumably, the

reason is that FFT is not sufficiently effective in quantifying dynamic signals as it requires a signal to be stationary during analysis of the whole interval.

The contingent negative variation (CNV), which is generally considered representative of an increase in neuronal excitability in neural networks in preparation for carrying out a task, and which is a useful index of learning¹⁶, was greater for CS⁺ than CS⁻ in each 500-ms time period after trial onset, and was significant at the somatosensory and motor electrode sites in the last two 500-ms time periods before shock onset ($F(1, 15) = 8.43$ and 6.59 , $P < 0.01$ and $P < 0.02$, respectively). The difference in evoked-response-potential waves between CS⁺ and CS⁻ (CS⁺ minus CS⁻) at each pericentral and posterior parietal site exhibiting increased gamma coherence with an occipital site (receiving the CSs) is shown in Fig. 2. The height of the upward (negative) deflection of these waves indicates the substantial extent to which the CNV to CS⁺ exceeded the response to CS⁻ (which was essentially zero at all electrode sites). The change in CNV resulting from the training supplements the change in colour-preference data (see Methods) as indicators, independent from the gamma-band data, that learning had taken place.

Our study, which is based on a previous classical conditioning/CNV study¹⁷, extends to associative learning, the process of greatest interest to Hebb, the phenomena to which gamma-band EEG activity may be related. Moreover, the formation of stable connections between different brain areas involved in the processing of stimuli presented to different sensory modalities during an associative-learning procedure is a good model of the formation of cell assemblies, as it provides an unambiguous and easily specified means of requiring that widely separated areas of the brain interact. It is of further interest that not only did gamma-band abundance increase in regions of the brain that received the two classes of stimuli involved in the training procedure, but gamma-band coherence also increased between them. Coherence or in-phase synchronicity is, in conceptual terms, the simplest and most straightforward process that could provide the basis for the formation of hebbian cell assemblies. The linkage or communication between visual cortex and somatosensory/motor cortex that was observed could have been direct, mediated by a third, intermediary region(s), or produced by the oscillation in a third region(s) that caused the gamma coherence in both areas. At the neuronal level, the mechanism could involve the recently discovered superficial pyramidal 'chattering cells' that may act as excitatory pacemakers for coherent gamma-band rhythms^{18,19} and/or the interconnected chaining of interneuronal networks operating to produce 'spike doublets'^{20,21}. It remains for future research to resolve these issues. Whatever the mechanism, however, it seems possible that the development of gamma coherence is involved not only in the establishment of associative learning, but also in other types of learning as well. □

Methods

The experiment was carried out in a sound-retarded, electrically shielded chamber. The subjects sat in a reclining chair and were asked to keep their arms relaxed on arm rests and their eyes open. They were paid for the test session, which took ~3 h.

Training. Intracutaneous electrical stimuli²² (10-ms duration) were used as painful UCS. Pain threshold was determined before the training phase by the method of limits using three pairs of ascending and descending series of stimulus intensities. Pain intensity was judged on a scale from 1 (not painful at all) to 12 (unbearably painful). The mean stimulation current of all trials for pain-threshold determination with an intensity rating of 5 was adopted as the pain threshold. Electrical stimulation intensity was set 40% above the physical value of the pain threshold.

EEG recording. EEG data were recorded from 31 Ag/AgCl electrodes mounted on the subject's scalp according to the international 10–20 system, with additional electrodes interspersed between standard electrode sites, and at left

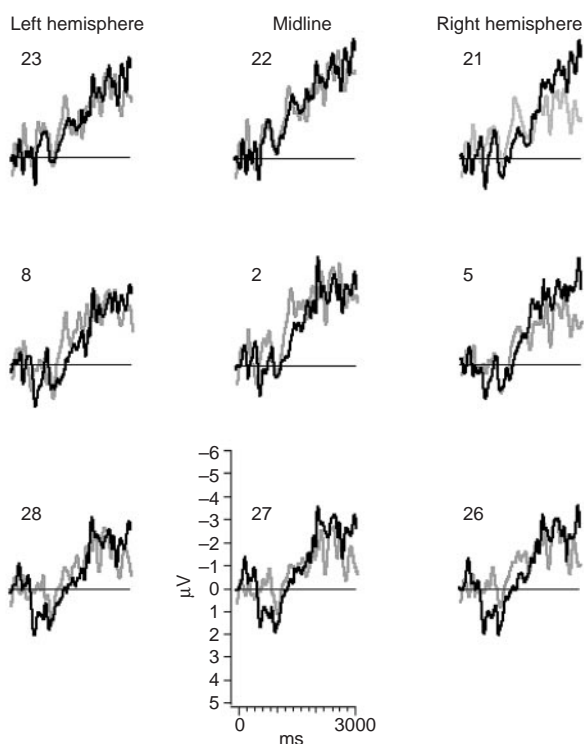


Figure 2 Difference in evoked-response-potential waves between CS⁺ and CS⁻ at each electrode involved in response to the UCS when the UCS was administered to the left (grey line) and right (black line) midfingers. A CNV (upward deflection of wave) developed at each of these electrode sites in the period before UCS presentation during CS⁺ but not CS⁻ (repeated-measures analysis of variance, all P values < 0.05). The CNV to the CS⁺ indicates readiness to respond to the UCS and that learning had taken place. The number in the top left corner of each panel indicates for what electrode in Fig. 1 the CNV waveforms are shown.

and right earlobes, as outlined in Fig. 1. Electrode Cz served as common reference. Vertical and horizontal electro-oculographic (EOG) data were recorded for eye blinks and eye movements. EEG and EOG data were collected for a total period of 4,250 ms, beginning 250 ms before visual-stimulus presentation and continuing for 1,000 ms after the end of a trial. EEG data were corrected for eye movements and eye blinks²³. Data were sampled online at 200 Hz using a time constant of 10 s.

Data analysis. For off-line data analysis, a current-source density (CSD) analysis was performed based on a spherical spline interpolation algorithm using two dimensional Laplace-operators and weighted Legendre polynomials^{24–26} in order to maximize the topographic specificity of electrical sources and sinks and to obtain reference-free measures for each electrode²⁴. Resulting CSD waveforms were then submitted to a method of coherence analysis involving time-varying autoregressive modelling of multivariate time series based on Kalman filtering^{15,27–28}. In the case of single-component signals the use of Kalman filters to fit autoregressive models with time-varying coefficients is common^{27–28}. This is possible because such signal models can be given in state-space form. As the Kalman filter can be designed for multi-component signals, we have used a similar state-space form for multi-component autoregressive models with time-varying coefficients. This enables an adaptive estimation of the autoregressive coefficients and derived spectral parameters (that is, coherence) which is suitable for the analysis of non-stationary signals. An order of 16 was chosen for the fitted autoregressive models.

Coherence was computed separately in the bandwidth 37–43 Hz (refs 2, 19), for the delta (0.6–3.5 Hz), theta (3.6–7.5 Hz), alpha 1 (7.6–10 Hz) and alpha 2 (10.1–12.5 Hz) frequency bands, and for additional bands between 30 and 36 Hz, 43 and 48 Hz, and 80 to 100 Hz for the 250-ms time window from 1,250 to 1,500 ms after stimulus onset and the window just before shock onset (that is, 2,750–3,000 ms after stimulus onset). This was also done for the raw EEG. The pairs of electrodes for which analysis was done covered the occipital area (CS⁺, CS⁻), the primary and association somatosensory projection areas (noxious stimulus), and the primary motor areas on both sides of the brain and at the midline. Gamma abundance was also calculated for the frequency band studied in refs 2, 6 (37–43 Hz). Coherence measures were transformed using Fisher's z-transformation and collapsed to obtain mean coherence measures for each subject, each pair of electrodes and each condition of visual stimulation.

Preference for colours of CS⁺ and CS⁻. Data on colour preference were obtained by questionnaire for the two colours (red and green) assigned randomly to CS⁺ and CS⁻ before, during, and at the end of acquisition and during and at the end of extinction. The colour-preference data were submitted to a repeated-measures analysis of variance and analysed as a function of condition (CS⁺, CS⁻), and time (beginning, during and end of acquisition, and during and end of extinction). Results were corrected for violation of sphericity using the Greenhouse–Geisser approach to epsilon correction of degrees of freedom. There was a significant effect for condition ($F(1, 18) = 6.64$, $P < 0.02$), time ($F(4, 72) = 10.43$, $P < 0.0001$, $e = 0.60$), and the condition \times time interaction ($F(4, 72) = 9.14$, $P < 0.0001$, $e = 0.751$), indicating that learning of the association between colour and electric shock had taken place. CS⁺ was perceived as most aversive during training, whereas during extinction the difference in preference for CS⁺ over CS⁻ had almost disappeared.

Received 12 October; accepted 1 December 1998.

1. Hebb, D. O. *The Organization of Behavior* (Wiley, New York, 1949).
2. Singer, W. & Gray, C. M. Visual feature integration and the temporal correlation hypothesis. *Annu. Rev. Neurosci.* **18**, 555–586 (1995).
3. Basar, E., Basar-Eroglu, C. & Schürmann, M. Sensory and cognitive components of brain resonance responses. *Acta Otolaryngol. (Stockh.)* **491**, 25–35 (1991).
4. Engel, A. K., König, P., Kreiter, A. K. & Singer, W. Interhemispheric synchronization of oscillatory neuronal responses in cat visual cortex. *Science* **252**, 1177–1179 (1991).
5. Pantev, C. Evoked and induced gamma-band activity of the human cortex. *Brain Topogr.* **7**, 321–330 (1995).
6. Singer, W. The formation of cooperative cell assemblies in the visual cortex. *J. Exp. Biol.* **153**, 177–197 (1990).
7. Pulvermüller, F., Lutzenberger, W., Preißl, H. & Birbaumer, N. Spectral responses in the gamma-band: physiological signs of higher cognitive processes? *Neuroreport* **6**, 2059–2064 (1995).
8. Murthy, V. N., Aoki, F. & Fetz, E. E. In *Oscillatory Event-Related Brain Dynamics* (eds Pantev, C., Elbert, T. & Lütkenhöner, B.) 213–226 (Plenum, New York, 1994).
9. Llinas, R. R. & Ribary, U. Coherent 40-Hz oscillation characterizes dream state in humans. *Proc. Natl. Acad. Sci. USA* **90**, 2078–2081 (1993).
10. Sheer, D. E. In *Self-regulation of the Brain and Behavior* (eds Elbert, T., Rockstroh, B., Lutzenberger, W. & Birbaumer, N.) 64–84 (Springer, Berlin, 1984).
11. Steriade, M., Amzica, F. & Contreras, D. Synchronization of fast (30–40 Hz) spontaneous cortical rhythms during brain activation. *J. Neurosci.* **16**, 392–417 (1996).

12. Tiitinen, H. et al. Selective attention enhances the auditory 40-Hz transient response in humans. *Nature* **364**, 59–60 (1993).
13. Oldfield, R. C. The assessment and analysis of handedness: the Edinburgh inventory. *Neuropsychology* **9**, 97–113 (1971).
14. Pulvermüller, F., Birbaumer, N., Lutzenberger, W. & Mohr, B. High-frequency brain activity: its possible role in attention, perception and language processing. *Prog. Neurobiol.* **52**, 427–445 (1997).
15. Arnold, M., Miltner, W. H. R., Bauer, R. & Braun, C. Adaptive AR modeling of nonstationary time series by means of Kalman filtering. *IEEE Trans. Biomed. Eng.* **45**, 553–562 (1998).
16. Rockstroh, B., Elbert, T., Canavan, A., Lutzenberger, W. & Birbaumer, N. *Slow Cortical Potentials and Behaviour* (Urban & Schwarzenberg, Munich, 1989).
17. Waschulewski Floruss, H., Miltner, W., Brody, S. & Braun, C. Classical conditioning of pain responses. *Int. J. Neurosci.* **78**, 21–32 (1994).
18. Gray, C. M. & McCormick, D. A. Chattering cells: superficial pyramidal neurons contributing to the generation of synchronous oscillations in the visual cortex. *Science* **274**, 109–113 (1996).
19. Gray, C. M., König, P., Engel, A. K. & Singer, W. Oscillatory responses in cat visual cortex exhibit inter-columnar synchronization which reflects global stimulus properties. *Nature* **338**, 334–337 (1989).
20. Jefferys, J. G., Traub, R. D. & Whittington, M. A. Neuronal networks for induced '40 Hz' rhythms. *Trends Neurosci.* **19**, 202–208 (1996).
21. Traub, R. D., Whittington, M. A., Stanford, I. M. & Jefferys, J. G. A mechanism for generation of long-range synchronous fast oscillations in the cortex. *Nature* **383**, 621–624 (1996).
22. Bromm, B. & Meier, W. The intracutaneous stimulus: a new pain model for algometric studies. *Meth. Find. Exp. Clin. Pharmacol.* **6**, 405–410 (1984).
23. Gratton, G., Coles, M. G. & Donchin, E. A new method for off-line removal of ocular artifact. *Electroencephalogr. Clin. Neurophysiol.* **55**, 468–484 (1983).
24. Perrin, F., Pernier, J., Bertrand, O. & Echallier, J. F. Spherical splines for scalp potential and current density mapping. *Electroencephalogr. Clin. Neurophysiol.* **72**, 184–187 (1989).
25. Biggins, C. A., Fein, G., Raz, J. & Amir, A. Artificially high coherences result from using spherical spline computation of scalp current density. *Electroencephalogr. Clin. Neurophysiol.* **79**, 413–419 (1991).
26. Perrin, F. Comments on article by Biggins et al. *Electroencephalogr. Clin. Neurophysiol.* **83**, 171–174 (1992).
27. Haykin, S. *Adaptive Filter Theory* (Prentice-Hall, Englewood Cliffs, New Jersey, 1986).
28. Chen, H. H. & Guo, L. *Identification and Stochastic Adaptive Control* (Birkhäuser, Boston, Massachusetts, 1991).

Acknowledgements. We thank I. Gutberlet for assistance in data analysis. This research was supported by a grant from the Deutsche Forschungsgemeinschaft to W.H.R.M. and a grant from the Rehabilitation Research and Development service, US Department of Veterans Affairs to E.T.

Correspondence and requests for materials should be addressed to W.H.R.M. (email: miltner@biopsy.uni-jena.de).

Origin of HIV-1 in the chimpanzee *Pan troglodytes troglodytes*

Feng Gao*, Elizabeth Bailes†, David L. Robertson‡, Yalu Chen*, Cynthia M. Rodenburg*, Scott F. Michael*§, Larry B. Cummins||, Larry O. Arthur†, Martine Peeters#, George M. Shaw*☆, Paul M. Sharp† & Beatrice H. Hahn*

* Departments of Medicine and Microbiology, University of Alabama at Birmingham, 701 S. 19th Street, LHRB 613, Birmingham, Alabama 35294, USA

† Institute of Genetics, University of Nottingham, Queens Medical Centre, Nottingham NG7 2UH, UK

‡ Laboratory of Structural and Genetic Information, CNRS, Marseilles 13402, France

§ Southwest Foundation for Biomedical Research, San Antonio, Texas 78245, USA

¶ AIDS Vaccine Program, National Cancer Institute-Frederick Cancer Research and Development Center, SAIC Frederick, Frederick, Maryland 21702, USA

Laboratoire Retrovirus, ORSTOM, BP 5045, Montpellier 34032, France

☆ Howard Hughes Medical Institute, University of Alabama at Birmingham, Birmingham, Alabama 35294, USA

The human AIDS viruses human immunodeficiency virus type 1 (HIV-1) and type 2 (HIV-2) represent cross-species (zoonotic) infections^{1–4}. Although the primate reservoir of HIV-2 has been clearly identified as the sooty mangabey (*Cercocebus atys*)^{2,4–7}, the origin of HIV-1 remains uncertain. Viruses related to HIV-1 have been isolated from the common chimpanzee (*Pan troglodytes*)^{8,9}, but only three such SIVcpz infections have been documented^{1,10,11}, one of which involved a virus so divergent¹¹ that it might represent a different primate lentiviral lineage. In a search for the HIV-1 reservoir, we have now sequenced the genome of a new SIVcpz

§ Present address: Department of Tropical Medicine, Tulane University, New Orleans, Louisiana 70112, USA.